

One-loop self-energy and counterterms in a massive Yang-Mills theory based on the nonlinearly realized gauge group

D. Bettinelli,^{*} R. Ferrari,⁺ and A. Quadri[‡]

Dipartimento di Fisica, Università degli Studi di Milano and INFN, Sezione di Milano, via Celoria 16, I-20133 Milano, Italy
(Received 13 September 2007; published 14 May 2008)

In this paper, we evaluate the self-energy of the vector mesons at one loop in our recently proposed subtraction scheme for the massive nonlinearly realized SU(2) Yang-Mills theory. We check the fulfillment of physical unitarity. The resulting self-mass can be compared with the value obtained in the massive Yang-Mills theory based on the Higgs mechanism, consisting in extra terms due to the presence of the Higgs boson (tadpoles included). Moreover, we evaluate all the one-loop counterterms necessary for the next order calculations. By construction, they satisfy all the equations of the model (Slavnov-Taylor, local functional equation, and Landau gauge equation). They are sufficient to make all the one-loop amplitudes finite through the hierarchy encoded in the local functional equation.

DOI: [10.1103/PhysRevD.77.105012](https://doi.org/10.1103/PhysRevD.77.105012)

PACS numbers: 11.10.Gh, 11.10.Lm, 11.15.Bt

I. INTRODUCTION

We have recently proposed a subtraction procedure [1] of the divergences in the SU(2) Yang-Mills (Y-M) theory [2] with a mass term [3–5] based on a nonlinearly realized gauge group. This theory has no Higgs boson in the perturbative approach.

The proposed subtraction scheme is based on the following strategy. i) A local functional equation is derived encoding a hierarchy among the 1-PI Green functions. According to this hierarchy, all of the amplitudes involving at least one unphysical Goldstone boson are fixed by the local functional equation once one knows the amplitudes independent of the Goldstone bosons (ancestor amplitudes). ii) It is shown that only a finite number of divergent ancestor amplitudes exists at every loop order (weak power-counting). iii) The subtraction of the divergences is based on dimensional regularization. In particular, the local functional equation indicates that only the poles in $D - 4$ should be removed in the properly normalized amplitudes.

Thus, the algorithm does not modify the number of the independent parameters of the zero-loop effective action. Hence, although the original Lagrangian is not renormalizable, we construct order by order in \hbar a consistent theory which depends on three parameters: the coupling constant g , the mass M and the mass scale Λ for the radiative corrections. The tree-level vertex functional compatible with the symmetry properties of the theory (Slavnov-Taylor, local functional equation and Landau gauge equation) and the weak power-counting is unique. This strategy is unconventional and departs from the standard renormalization procedure.

The proof of consistency (in the iterative subtraction) has been given in a series of papers [1,5–10]. In particular, the Slavnov-Taylor identity [11] is maintained after the counterterms are introduced. The same is valid for the local functional equation (LFE) derived from the transformation properties under local left multiplication as well as for the Landau gauge equation.

Physical unitarity is guaranteed to follow from the Slavnov-Taylor identity [12,13]. Locality of the counterterms follows from the above mentioned local functional equation. The construction of the counterterms is based on two important properties of this equation: hierarchy and weak power-counting, which allow a full control of the amplitudes involving the auxiliary scalar fields (descendant) in terms of the amplitudes with no auxiliary fields (ancestor).

In this work, we provide as an example the evaluation of the self-energy of the vector meson in D dimensions by using the Landau gauge. This explicit calculation is necessary for the following reasons: i) to show how the proposed subtraction procedure works; ii) to check that the Landau gauge (because of its unphysical pole at zero mass) does not pose any problem for physical unitarity as it is required for the proof given in Ref. [13]; and iii) to provide the quantitative difference between the theories with the linear (with Higgs boson) and the nonlinear representation (no Higgs boson) of the gauge group.

The result shows how physical unitarity is recovered on shell. A comparison with the theory where the gauge group is linearly realized (Higgs mechanism [14]) is very interesting. It shows that our approach yields a consistent identification of the Higgs part. This can be done on the physically relevant part: the self-mass of the vector meson. The discussion of this item necessitates the comparison of our calculation with previous works [15] usually employing a 't Hooft gauge [16]. Since the tadpoles (vacuum expectation value of the Higgs field) are gauge dependent,

^{*}daniele.bettinelli@mi.infn.it

⁺ruggero.ferrari@mi.infn.it

[‡]andrea.quadri@mi.infn.it

then the comparison can be made only for the self-mass. The identification of the Higgs contribution, up to the mass scale Λ , is possible because our approach does not allow the introduction of free parameters for each local invariant solution of the defining equations. These solutions for the one-loop case are listed in Appendix A.

The self-energy of the vector boson can be evaluated at the two-loop level. This calculation necessitates of the local one-loop counterterms. In this paper, we evaluate all the counterterms necessary for any two-loop calculation. This amounts to find the coefficients of the pole parts in $D - 4$ for all the ancestor amplitudes, i.e. for all external legs A_μ , V_μ , K_0 , Θ_μ , c , \bar{c} , and A_μ^* , c^* , ϕ^* , ϕ_0^* . Counterterms with Goldstone boson external legs are obtained from those involving only ancestor variables. They satisfy the linearized Slavnov-Taylor (ST) identity, the linearized LFE, and the Landau gauge equation. These constraints imply nontrivial relations among the ancestor amplitudes in the sector spanned by the external sources and the ghost field. Finally, the counterterms are described by a suitable basis of invariant local solutions of the same equations. Their coefficients are evaluated from the divergent part of the ancestor amplitudes. The latter are collected in Appendix B.

II. EFFECTIVE ACTION AT THE TREE LEVEL AND COUNTERTERMS

The Feynman rules are implicitly given by the vertex functional at the tree level

$$\begin{aligned} \Gamma^{(0)} = \frac{\Lambda^{(D-4)}}{g^2} \int d^D x \left\{ -\frac{1}{4} G_{a\mu\nu} G_a^{\mu\nu} + \frac{M^2}{2} (A_{a\mu} - F_{a\mu})^2 \right. \\ + B_a (D^\mu [V] (A_\mu - V_\mu))_a - \bar{c}_a (D^\mu [V] D_\mu [A] c)_a \\ + \Theta_a^\mu (D_\mu [A] \bar{c})_a + (A_{a\mu}^* s A_a^\mu + \phi_0^* s \phi_0 \\ \left. + \phi_a^* s \phi_a + c_a^* s c_a + K_0 \phi_0) \right\}, \quad (1) \end{aligned}$$

where, beside the conventional notations, B_a is the Lagrange multiplier for the Landau gauge, $V_{a\mu}$, $\Theta_{a\mu}$, K_0 are the external sources necessary for the LFE and $A_{a\mu}^*$, ϕ_0^* , ϕ_a^* , c_a^* are the antifields for the Becchi-Rouet-Stora-Tyutin-transforms sA_a^μ , $s\phi_0$, $s\phi_a$, sc_a . The mass scale Λ enters as a common factor in order to simplify the subtraction procedure. The nonlinearity of the representation of the gauge group $SU(2)_{\text{LEFT LOCAL}} \otimes SU(2)_{\text{RIGHT GLOBAL}}$ comes from the constraint on ϕ_0

$$\begin{aligned} F_{a\mu} \frac{\tau_a}{2} = F_\mu = i\Omega \partial_\mu \Omega^\dagger \\ \Omega_{ij} = \frac{1}{v} (\phi_0 + i\tau_a \phi_a)_{ij} \in SU(2) \\ \phi_0 = \sqrt{v^2 - \vec{\phi}^2}. \end{aligned} \quad (2)$$

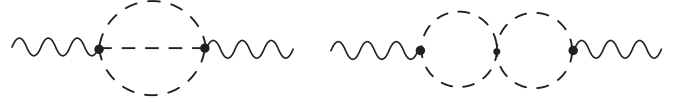


FIG. 1. Two-loop graphs where the nonlinearity appears. The dashed lines are $\vec{\phi}$.

The complete set of Feynman rules includes the counterterms

$$\hat{\Gamma} \equiv \Gamma^{(0)} + \frac{\Lambda^{(D-4)}}{g^2} \sum_{j \geq 1} \int d^D x \mathcal{M}^{(j)}. \quad (3)$$

The counterterms $\mathcal{M}^{(j)}$ are given by the pole parts in $D - 4$ of the normalized vertex functional [the normalization is tightly conditioned by the particular form of the effective action in Eq. (1)]

$$\int d^D x \mathcal{M}^{(j)} = - \frac{g^2}{\Lambda^{(D-4)}} \sum_{k=0}^{j-1} \Gamma^{(j,k)} \Big|_{\text{POLE PARTS}}, \quad (4)$$

where $\Gamma^{(j,k)}$ denotes the vertex functional where the total power of \hbar of the inserted counterterms is k . The subtraction procedure is consistent if the counterterms are local and if the relevant equations are preserved: Slavnov-Taylor, LFE, and Landau gauge equations. We have given the formal proofs that the subtraction proposed in Eq. (3) works for the Feynman rules in Eq. (1) [1]. In the present paper, we provide an explicit one-loop calculation. The result will be compared with the result of the linear theory (Higgs mechanism). In our final formula it is evident how physical unitarity is realized and how the parameter v of Eq. (2) disappears from the final result since it is not a physical parameter [1].

We provide also all the one-loop counterterms for the ancestor amplitudes (those with no ϕ -external legs). A complete two-loop calculation is expected to be a straightforward task, without any obstruction in the subtraction procedure, since the structure of the divergences is, for most graphs, that of the linear theory. There are few exceptions as those depicted in Fig. 1, which however have been already consistently dealt with in the nonlinear sigma model [6].

III. SELF-ENERGY FOR THE NONLINEAR MASSIVE Y-M

We give here the complete result of the one-loop calculation in D dimensions, without any subtractions. The graphs are shown in Fig. 2. The transverse part is

$$\begin{aligned} \Sigma_T(p^2) = & -\frac{i}{D-1} \left\{ H_1(M^2) \left[-2(D-1)^2 + 2D - \frac{5}{2} + (2D-3) \frac{p^2}{M^2} - \frac{p^2}{2M^2} \left(1 - \frac{M^2}{p^2} \right)^2 \right] \right. \\ & + H_2(M^2, M^2) \left[(-2D+3) \frac{p^4}{M^2} + (7D-10)p^2 + 4(D-1)M^2 - p^2 \left(\frac{p^2}{2M^2} - 1 \right)^2 \right] \\ & \left. + H_2(M^2, 0) \left[\left(M^2(2D-3) + \frac{p^2}{2} \right) \left(\frac{p^2}{M^2} - 1 \right)^2 + \frac{p^2}{2} \left(1 - \frac{M^2}{p^2} \right)^2 \right] + \frac{p^2}{4} \left(1 - \frac{p^4}{M^4} \right) H_2(0, 0) \right\}, \end{aligned} \quad (5)$$

where

$$\begin{aligned} H_1(m^2) &= \int_{\mathcal{M}} \frac{d^D q}{(2\pi)^D} \frac{1}{(q^2 - m^2)} \\ H_2(m_1^2, m_2^2) &= \int_{\mathcal{M}} \frac{d^D q}{(2\pi)^D} \frac{1}{(q^2 - m_1^2)[(p-q)^2 - m_2^2]}. \end{aligned} \quad (6)$$

The longitudinal part is

$$\begin{aligned} \Sigma_L(p^2) = & -iH_1(M^2) \left(\frac{3}{2} - \frac{p^2}{2M^2} \right) + i \frac{p^2}{2} \left(1 - \frac{M^2}{p^2} \right)^2 \\ & \times \left[H_2(M^2, 0) - \frac{1}{M^2} H_1(M^2) \right] - i \frac{p^2}{2} H_2(0, 0). \end{aligned} \quad (7)$$

It is worth to notice some points:

- (1) $\Sigma_T(0) = \Sigma_L(0)$ is verified for generic D . By this property the pole at $p^2 = 0$ in the 1-PI two-point function is avoided. This condition is very important in order to prove physical unitarity in the Landau gauge [13].
- (2) For $p^2 = M^2$, Σ_T contains only $H_2(M^2, M^2)$ which is the only Feynman integral with a physical discontinuity across the real positive p^2 axis.
- (3) As a check on $\Sigma_L(p^2)$, the relevant Slavnov-Taylor identity is explicitly evaluated in Appendix C.

The self-mass around $D = 4$ can be evaluated according to the prescription of Eq. (4). One gets

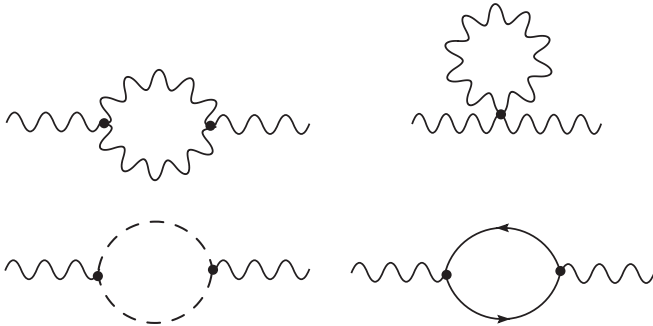


FIG. 2. Graphs of self-energy for the nonlinear theory. The arrows are for Faddeev-Popov ghosts.

$$\begin{aligned} g^2 \Sigma_T(M^2)|_{D \sim 4} = & g^2 \frac{M^2}{(4\pi)^2} \left\{ -\frac{23}{4} C_\Lambda + \frac{2}{3} - \frac{33}{4} \right. \\ & \left. \times \int_0^1 dx P(1, x) \right\} \end{aligned} \quad (8)$$

with

$$C_\Lambda \equiv \frac{2}{D-4} + \gamma - \ln 4\pi + \ln \left(\frac{M^2}{\Lambda^2} \right) \quad (9)$$

and

$$P(r, x) \equiv x^2 - rx + r. \quad (10)$$

IV. SELF-ENERGY IN THE LINEAR THEORY

At one loop it is straightforward to evaluate the contribution of the Higgs sector. By this we mean the contribution of the graphs in Fig. 3. Our approach fixes the separation of the Higgs from the non-Higgs contribution once Λ is given. This is at variance with other approaches where the Higgs part is removed by hand. In these methods, the arbitrariness introduced at one loop is due to the presence of free parameters associated to the local solutions of the ST identity and of the linearized LFE, once the logs of M_H are removed by hand. This problem has been discussed thoroughly in Refs. [9,10] for the nonlinear sigma model. The nondecoupling effects in the large Higgs mass limit have been studied at length in the literature [see e.g. Refs. [17] for the standard model and [18] for the SU(2) case].

The Higgs contribution to the self-energy is evaluated in the Landau gauge by using the same form for the effective action of Eq. (1) without the constraint in Eq. (2). The mass term becomes ($\phi_0 = h + v$)

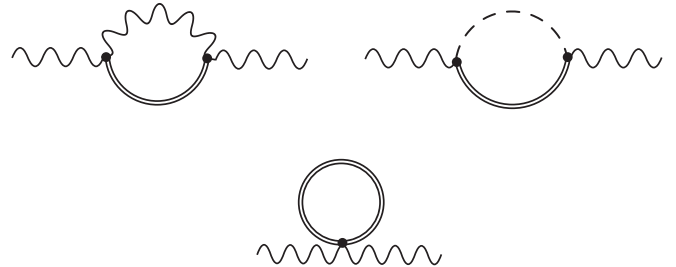


FIG. 3. Graphs of self-energy for the linear theory (involving a Higgs line).

$$\begin{aligned}
\frac{M^2}{2}(A_{a\mu} - F_{a\mu})^2 &= M^2 \text{Tr}(A_\mu - i\Omega \partial_\mu \Omega^\dagger)^2 \\
&= M^2 \text{Tr}\{[\Omega^\dagger A_\mu - i\partial_\mu \Omega^\dagger][A_\mu \Omega + i\partial_\mu \Omega]\} \\
&= \frac{4M^2}{v^2} \left\{ \frac{1}{2} \partial_\mu h \partial^\mu h + \frac{1}{2} \partial_\mu \phi_a \partial^\mu \phi_a + \frac{1}{8} A^2 (h^2 + 2vh + v^2 + \vec{\phi}^2) \right. \\
&\quad \left. + \frac{1}{2} A_a^\mu [\partial_\mu h \phi_a - (h + v) \partial_\mu \phi_a + \epsilon_{abc} \phi_b \partial_\mu \phi_c] \right\}
\end{aligned} \tag{11}$$

and the potential is added

$$\begin{aligned}
-\frac{\lambda^2}{4}(h^2 + \vec{\phi}^2 + 2vh)^2 &= -\lambda^2 v^2 h^2 - \frac{\lambda^2}{4}(h^4 + \vec{\phi}^4 \\
&\quad + 2h^2 \vec{\phi}^2 + 4vh^3 + 4vh \vec{\phi}^2).
\end{aligned} \tag{12}$$

The Higgs mass is

$$M_H^2 = \frac{\lambda^2 v^4}{2M^2}. \tag{13}$$

By using these Feynman rules, the contribution of the graphs in Fig. 3 is evaluated. The contribution of the Higgs to the transverse part of the two-point function is

$$\begin{aligned}
\Sigma_T^{\text{HIGGS}}(p^2) &= -\frac{i}{4} \frac{1}{(D-1)} \left\{ H_1(M_H^2) \left(\frac{M_H^2}{p^2} - \frac{M^2}{p^2} + 2 - D \right) \right. \\
&\quad - H_2(M^2, M_H^2) \left[4(D-2)M^2 \right. \\
&\quad \left. \left. + \frac{(p^2 + M^2 - M_H^2)^2}{p^2} \right] \right. \\
&\quad \left. + H_1(M^2) \left(\frac{M^2}{p^2} - \frac{M_H^2}{p^2} + 1 \right) \right\}.
\end{aligned} \tag{14}$$

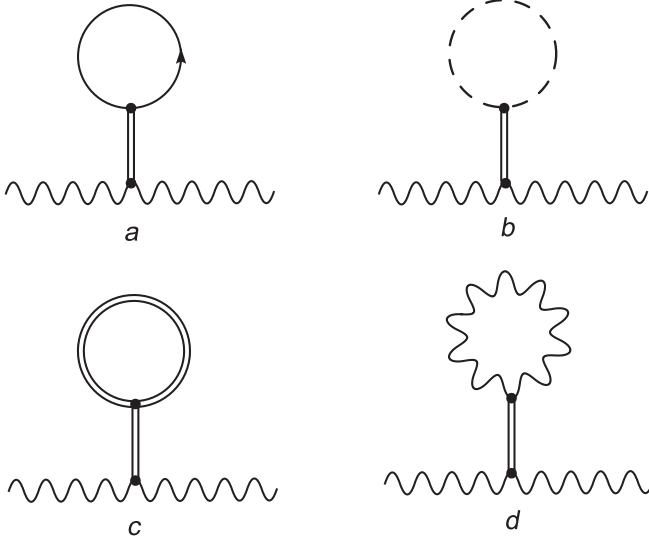


FIG. 4. Tadpoles originated from the nonzero vacuum expectation value of ϕ_0 . (a) and (b) (tadpoles of the Faddeev-Popov ghosts and of the Goldstone boson) are zero for massless Goldstone bosons.

The contribution of the Higgs sector to the longitudinal part of the two-point function is

$$\begin{aligned}
\Sigma_L^{\text{HIGGS}}(p^2) &= -\frac{i}{4} \left[\frac{M^2 - M_H^2}{p^2} H_1(M_H^2) \right. \\
&\quad - \frac{p^2 + M^2 - M_H^2}{p^2} H_1(M^2) \\
&\quad \left. + \left[\frac{(p^2 + M^2 - M_H^2)^2}{p^2} \right. \right. \\
&\quad \left. \left. - 4M^2 \right] H_2(M^2, M_H^2) + (2M_H^2 \right. \\
&\quad \left. - p^2) H_2(M_H^2, 0) \right].
\end{aligned} \tag{15}$$

For later discussion, let us remind the reader that Eqs. (14) and (15) are the contribution of the Higgs sector (in the linear theory) to the self-energy of the vector meson in the Landau gauge. The graphs shown in Fig. 4 have to be included as a contribution coming from the Higgs sector. In fact, we want to compare the predictions in the linear and nonlinear realization of the gauge group. Thus, no finite subtraction is performed and the parameters entering in the self-mass (g and M) are given by the zero-order values. In the Landau gauge both graphs (a) and (b) in Fig. 4 are zero. Then we have

$$\begin{aligned}
\Sigma_T^{\text{TADPOLES}}(p^2) &= \Sigma_L^{\text{TADPOLES}}(p^2) \\
&= -\frac{3i}{4} H_1(M_H^2) - \frac{3i}{2} \frac{M^2}{M_H^2} (D-1) H_1(M^2).
\end{aligned} \tag{16}$$

V. SELF-MASS IN THE NONLINEAR VERSUS LINEAR

The results of the Secs. III and IV allow a comparison of the self-mass in the two cases. The subtraction procedure of the poles in $D-4$ must be the same. However, this is not enough. In the linear case, a finite renormalization is always possible, and, in particular, it is possible to drop the tadpole contributions, since they can be eventually accounted for by some mass counterterms. A comparison between the theories based on the linear and the nonlinear representation of the gauge group necessitates that the parameters g and M enter as zero-order values and not as

dummy variables. In fact, the counterterms can be even gauge-dependent if they are introduced in order to balance the dropping of the tadpoles (see next section).

Now we take the case $p^2 = M^2$ of Σ_T and then consider the Laurent expansion around $D = 4$. We have in the nonlinear case from Eq. (8)

$$\delta M_{\text{NONLINEAR}}^2 = \frac{g^2 M^2}{(4\pi)^2} \left\{ -\frac{23}{4} C_\Lambda + \frac{2}{3} - \frac{33}{4} \times \int_0^1 dx P(1, x) \right\}. \quad (17)$$

The linear theory, based on the Higgs mechanism, adds to the above term the following quantity (tadpoles of Fig. 4 are included)

$$\begin{aligned} \delta M_{\text{LINEAR}}^2 = \delta M_{\text{NONLINEAR}}^2 + \frac{g^2 M^2}{4 (4\pi)^2} & \left\{ \left(\frac{10}{3} - 3r - \frac{18}{r} \right) C_\Lambda \right. \\ & + \frac{10}{9} + \frac{6}{r} + \frac{7}{3}r + \frac{r^2}{3} - \left(2r + \frac{r^2}{3} \right) \ln r \\ & \left. + \left(4 - \frac{4}{3}r + \frac{r^2}{3} \right) \int_0^1 dx \ln P(r, x) \right\}, \quad (18) \end{aligned}$$

where

$$r = M^{-2} M_H^2. \quad (19)$$

VI. $\langle 0 | \phi_0 | 0 \rangle$ IS GAUGE DEPENDENT

The comparison of our calculation, given in Eqs. (17) and (18), with results present in the literature needs some consideration about gauge invariance of the vacuum. Thus, we use the 't Hooft gauge-fixing for the linear theory

$$\begin{aligned} \mathcal{L}'_{\text{'t Hooft}} = \frac{B_a^2}{2\alpha} + B_a \left(\partial A_a + \frac{2M^2}{v\alpha} \phi_a \right) - \bar{c}_a \left(\partial^\mu D[A]_{ab\mu} \right. \\ \left. + \frac{M^2}{v\alpha} (\phi_0 \delta_{ab} - \epsilon_{abc} \phi_c) \right) c_b. \quad (20) \end{aligned}$$

Hereafter, we list the amplitudes for the tadpoles in Fig. 4

$$\begin{aligned} \Sigma_{aa'\mu\nu}^{\text{TADPOLE FP}}(p) &= \frac{3i}{2} \frac{1}{\alpha} \frac{M^2}{M_H^2} g_{\mu\nu} \delta_{aa'} H_1 \left(\frac{M^2}{\alpha} \right) \\ &\sim \frac{3}{2} \frac{1}{\alpha} \frac{M^2}{M_H^2} g_{\mu\nu} \delta_{aa'} \frac{M^2}{\alpha (4\pi)^2} \left(\frac{2}{D-4} - 1 \right. \\ &\quad \left. + \gamma - \ln 4\pi + \ln \frac{M^2}{\alpha \Lambda^2} \right) \quad (21) \end{aligned}$$

$$\begin{aligned} \Sigma_{aa'\mu\nu}^{\text{TADPOLE GOLDSTONE}}(p) &= -\frac{3i}{4} g_{\mu\nu} \delta_{aa'} H_1 \left(\frac{M^2}{\alpha} \right) \\ &\sim -\frac{3}{4} g_{\mu\nu} \delta_{aa'} \frac{M^2}{\alpha (4\pi)^2} \left(\frac{2}{D-4} - 1 \right. \\ &\quad \left. + \gamma - \ln 4\pi + \ln \frac{M^2}{\alpha \Lambda^2} \right) \quad (22) \end{aligned}$$

$$\begin{aligned} \Sigma_{aa'\mu\nu}^{\text{TADPOLE HIGGS}}(p) &= -\frac{3i}{4} g_{\mu\nu} \delta_{aa'} H_1(M_H^2) \\ &\sim -\frac{3}{4} g_{\mu\nu} \delta_{aa'} \frac{M_H^2}{(4\pi)^2} \left(\frac{2}{D-4} - 1 + \gamma \right. \\ &\quad \left. - \ln 4\pi + \ln \frac{M_H^2}{\Lambda^2} \right) \quad (23) \end{aligned}$$

$$\begin{aligned} \Sigma_{aa'\mu\nu}^{\text{TADPOLE GAUGE}}(p) &= -\frac{3i}{2} \frac{M^2}{M_H^2} g_{\mu\nu} \delta_{aa'} \left((D-1) H_1(M^2) + \frac{1}{\alpha} H_1 \left(\frac{M^2}{\alpha} \right) \right) \\ &\sim -\frac{3}{2} \frac{M^2}{M_H^2} g_{\mu\nu} \delta_{aa'} \left\{ (D-1) \frac{M^2}{(4\pi)^2} \left(\frac{2}{D-4} - 1 + \gamma - \ln 4\pi + \ln \frac{M^2}{\Lambda^2} \right) \right. \\ &\quad \left. + \frac{1}{\alpha} \frac{M^2}{\alpha (4\pi)^2} \left(\frac{2}{D-4} - 1 + \gamma - \ln 4\pi + \ln \frac{M^2}{\alpha \Lambda^2} \right) \right\}. \quad (24) \end{aligned}$$

It is amazing that

$$\begin{aligned} \Sigma_{aa'\mu\nu}^{\text{TADPOLE GAUGE}}(p) + \Sigma_{aa'\mu\nu}^{\text{TADPOLE FP}}(p) \\ = -\frac{3i}{2} \frac{M^2}{M_H^2} g_{\mu\nu} \delta_{aa'} (D-1) H_1(M^2) \quad (25) \end{aligned}$$

is gauge independent. Moreover,

$$\begin{aligned} \langle 0 | \phi_0 | 0 \rangle = v \left\{ 1 - \frac{g^2}{2M^2} \frac{1}{\Lambda^{(D-4)}} \frac{3i}{4} \left[H_1(M_H^2) \right. \right. \\ \left. \left. + 2 \frac{M^2}{M_H^2} (D-1) H_1(M^2) + H_1 \left(\frac{M^2}{\alpha} \right) \right] \right\}, \quad (26) \end{aligned}$$

i.e. the vacuum expectation value of ϕ_0 is gauge dependent through the mass of the Goldstone boson $\frac{M^2}{\alpha}$.

The above discussion shows that tadpoles have to be considered in the evaluation of the self-mass if one wants a gauge-invariant result. In the linear theory, it is not compelling to introduce the tadpoles, since one can always perform a finite renormalization in order to restore gauge invariance. However, with this choice, one is not allowed to use the physical parameters for the zero-order-value entries of g , M , and M_H .

The comparison of our results with the expression given by Marciano and Sirlin in Appendix A of Ref. [15] must take into account these facts. Their result for the gauge

group $SU(2)$ ¹

$$A(M^2)_{AA}^{\text{MARCIANO SIRLIN}} = \frac{g^2 M^2}{16\pi^2} \left\{ -\frac{25}{6} C_\Lambda + \frac{7}{36} - \frac{1}{6} \left(r - \frac{r^2}{2} \right) - \frac{r^2}{12} \ln r + \frac{r}{4} \ln r - \frac{33}{4} \int_0^1 \ln P(1, x) + \left(\frac{r^2}{12} - \frac{r}{3} + 1 \right) \int_0^1 dx P(r, x) \right\} \quad (27)$$

must be complemented by the contribution of the tadpole (b) in Fig. 4 (at $\alpha = 1$) in order to get a gauge-invariant result

$$A(M^2)_{AA}^{\text{MARCIANO SIRLIN}} + \Sigma^{\text{TADPOLE GOLDSTONE}} = \frac{g^2 M^2}{16\pi^2} \left\{ -\frac{59}{12} C_\Lambda + \frac{34}{36} - \frac{1}{6} \left(r - \frac{r^2}{2} \right) - \frac{r^2}{12} \ln r + \frac{r}{4} \ln r - \frac{33}{4} \int_0^1 \ln P(1, x) + \left(\frac{r^2}{12} - \frac{r}{3} + 1 \right) \int_0^1 dx P(r, x) \right\}. \quad (28)$$

This agrees with our results in Eq. (18) if we add to the expression in Eq. (28) the contributions of the gauge, Higgs, and Faddeev-Popov tadpoles as reported in Eqs. (23) and (25).

VII. ONE-LOOP COUNTERTERMS

Two-loop calculations require the knowledge of the full set of one-loop counterterms. The counterterms must obey the ST identity, the local functional equation, and the Landau gauge equation [1]. According to the hierarchy property, only the counterterms involving ancestor variables have to be computed in order to implement the iterative subtraction of the divergences. The full list of the relevant invariant solutions is reported in Appendix A specialized to the case where the descendant fields are neglected (Goldstone boson fields). Counterterms involving descendant field external legs are obtainable by using the full expression of the invariant solutions given in Ref. [1]: the compact expressions, written in terms of bleached fields, must be projected on the relevant monomials.

The coefficients of the invariants are determined by computing the divergent part of the relevant ancestor amplitudes after the proper normalization given by Eq. (4).

¹This equation has been obtained by using the identity

$$\int_0^1 dx P(r, x) \ln P(r, x) = \frac{1}{3} \left(-\frac{2}{3} + r - \frac{r^2}{2} + \frac{r^2}{2} \ln r - \left(\frac{r^2}{2} - 2r \right) \times \int_0^1 \ln P(r, x) \right).$$

The divergences of the ancestor amplitudes are collected in Appendix B.

One finds

$$\hat{\Gamma}^{(1)} = \frac{\Lambda^{(D-4)}}{(4\pi)^2} \frac{1}{D-4} \left[\frac{17}{2} (I_1 - I_2) - \frac{67}{6} I_3 + \frac{11}{4} I_4 - \frac{5}{2} I_5 + 3M^2 I_6 - 6I_7 + \frac{3v^2}{128M^4} I_8 - \frac{v}{8M^2} I_9 \right]. \quad (29)$$

I_{10} and I_{11} do not enter into the parametrization of the one-loop counterterms. This is a peculiar property of the Landau gauge.

It is clear from Eq. (29) that the one-loop counterterms for the pure gauge sector cannot be casted in the form

$$I_1 - I_2 - 2I_3 + I_4 - I_5 = \frac{1}{4} \int d^D x G_a^{\mu\nu} G_{a\mu\nu}, \quad (30)$$

as noted already in the early works on the divergences of the pure massive Y-M theory [19] [20]. Our approach allows one to overcome this difficulty by managing the divergences with another set of tools based both on Becchi-Rouet-Stora-Tyutin transformations and the invariance of the path integral measure under local left multiplication.

Despite the fact that they are divergent by power-counting, one-loop 1-PI amplitudes involving more than one V leg are finite. This result can be established from Eq. (29) by noticing that the dependence of $\hat{\Gamma}^{(1)}$ on V is only linear (via the invariant I_7).

VIII. CONCLUSIONS

In this paper we have provided the D -dimensional self-energy of the vector meson in the $SU(2)$ gauge group in the nonlinearly realized perturbative formulation recently proposed in [1]. We have discussed how physical unitarity is recovered on shell and presented a comparison with the linear theory. Such a comparison is possible since the subtraction scheme of [1] allows one to separate the Higgs part of the self-mass. This is a consequence of the fact that in our approach no free parameters can be introduced for each local invariant solution of the defining equations, as listed in Appendix A for the one-loop case. We have also given the full set of one-loop counterterms which are required for any two-loop computation. The counterterms have been parametrized in terms of invariant solutions of the ST identity, the LFE, and the Landau gauge equation. Their coefficients are obtained from the evaluation of the divergent part of the ancestor amplitudes (no Goldstone fields).

ACKNOWLEDGMENTS

We are indebted to Glenn Barnich and Stefan Dittmaier for very stimulating discussions. We acknowledge a partial financial support by MIUR.

APPENDIX A: ONE-LOOP INVARIANTS

We list here the 11 invariants compatible with the symmetry requirements and the weak power-counting at the one-loop level. By the Landau gauge equation the depen-

dence of $\Gamma^{(1)}$ on \bar{c}_a happens in the combination

$$\hat{A}_{a\mu}^* = A_{a\mu}^* + (D_\mu[V]\bar{c})_a. \quad (\text{A1})$$

We neglect the descendant fields

$$\begin{aligned} I_1 &= \frac{1}{2} \int d^D x \partial_\mu A_{a\nu} \partial^\mu A_a^\nu, & I_2 &= \frac{1}{2} \int d^D x (\partial A_a)^2, & I_3 &= -\frac{1}{2} \int d^D x \epsilon_{abc} \partial_\mu A_{a\nu} A_b^\mu A_c^\nu, \\ I_4 &= \frac{1}{4} \int d^D x (A^2)^2, & I_5 &= \frac{1}{4} \int d^D x (A_{a\mu} A_b^\mu)(A_{a\nu} A_b^\nu), & I_6 &= \frac{1}{2} \int d^D x A^2, \\ I_7 &= \frac{1}{2} \int d^D x V_a^\mu (D^\rho G_{\rho\mu}[A] + M^2 A_\mu)_a - \frac{1}{2} \int d^D x \hat{A}_{a\mu}^* \Theta_a^\mu + \frac{1}{2} \int d^D x \hat{A}_{a\mu}^* (D^\mu[V]c)_a, & & & & (\text{A2}) \\ I_8 &= \int d^D x (2K_0 - c_a \phi_a^*)^2, & I_9 &= \int d^D x \left(\frac{1}{2} c_a \phi_a^* A^2 - K_0 A^2 \right), \\ I_{10} &= \int d^D x \left(\frac{1}{2} (D^\mu[A] \hat{A}_\mu^*)_a c_a - \frac{1}{4} \phi_a^* c_a - \frac{1}{2} c_a^* \epsilon_{abc} c_b c_c \right), & I_{11} &= \int d^D x (c_a \phi_a^* - 2K_0). \end{aligned}$$

We remind, once again, that $I_1 - I_{11}$ are not solutions of the ST identity, local functional equation, and Landau gauge equation. Instead, they are the projection on the ancestor variables of the solutions given in Ref. [1].

APPENDIX B: ONE-LOOP DIVERGENCES OF THE ANCESTOR AMPLITUDES

In this Appendix, we give the one-loop divergent parts of the ancestor amplitudes. The resulting counterterms are for the theory where the gauge group is represented nonlinearly and in the Landau gauge. The Feynman rules are encoded in Eq. (1). From that action we can read immediately the free propagators (the factor $\frac{g^2}{\Lambda^{(D-4)}}$ is always left understood)

$$\begin{aligned} \text{Wavy line} & \quad \Delta_{A_{a\mu} A_{b\nu}} = \frac{-i}{p^2 - M^2} \left(g_{\mu\nu} - \frac{p_\mu p_\nu}{p^2} \right) \delta_{ab} \\ \text{Dashed line} & \quad \Delta_{\phi_a \phi_b} = \frac{i}{4} \frac{v^2}{M^2} \frac{1}{p^2} \delta_{ab} \end{aligned}$$

$$\begin{aligned} \text{Wavy line with dot} & \quad \Delta_{B_a A_{b\mu}} = \frac{p_\mu}{p^2} \delta_{ab} \\ \text{Dashed line with dot} & \quad \Delta_{B_a \phi_b} = -i \frac{v}{2p^2} \delta_{ab} \\ \text{Arrow} & \quad \Delta_{c_a \bar{c}_b} = \frac{i}{p^2} \delta_{ab} \\ \text{Solid line} & \quad \Delta_{B_a B_b} = 0 \\ \text{Wavy line with dot and dashed line} & \quad \Delta_{\phi_a A_{b\mu}} = 0. \end{aligned}$$

We list here the relevant vertices for the one-loop divergent ancestor amplitudes (the factor $\frac{\Lambda^{(D-4)}}{g^2}$ is always left understood)

$$\begin{aligned} i\Gamma_{A_a^\mu(p_1) A_b^\nu(p_2) A_c^\rho(p_3)}^{(0)} &= -\epsilon_{abc} [g_{\mu\nu}(p_1 - p_2)_\rho + g_{\mu\rho}(p_3 - p_1)_\nu + g_{\nu\rho}(p_2 - p_3)_\mu] \\ i\Gamma_{A_a^\mu(p_1) A_b^\nu(p_2) A_c^\rho(p_3) A_d^\eta(p_4)}^{(0)} &= -i [\delta_{ab} \delta_{cd} (2g_{\mu\nu} g_{\rho\eta} - g_{\mu\rho} g_{\nu\eta} - g_{\mu\eta} g_{\nu\rho}) + \delta_{ac} \delta_{bd} (-g_{\mu\nu} g_{\rho\eta} + 2g_{\mu\rho} g_{\nu\eta} - g_{\mu\eta} g_{\nu\rho}) \\ &\quad + \delta_{ad} \delta_{bc} (-g_{\mu\nu} g_{\rho\eta} - g_{\mu\rho} g_{\nu\eta} + 2g_{\mu\eta} g_{\nu\rho})] \\ i\Gamma_{A_a^\mu(p_1) \phi_b(p_2) \phi_c(p_3)}^{(0)} &= \frac{2M^2}{v^2} \epsilon_{abc} (p_2 - p_3)_\mu & i\Gamma_{A_a^\mu(p_1) V_b^\nu(p_2) B_c(p_3)}^{(0)} &= -i \epsilon_{abc} g_{\mu\nu} & i\Gamma_{A_a^\mu(p_1) c_b(p_2) \bar{c}_c(p_3)}^{(0)} &= \epsilon_{abc} p_{3\mu} \\ i\Gamma_{V_a^\mu(p_1) c_b(p_2) \bar{c}_c(p_3)}^{(0)} &= -\epsilon_{abc} p_{2\mu} & i\Gamma_{A_a^\mu(p_1) V_b^\nu(p_2) c_c(p_3) \bar{c}_d(p_4)}^{(0)} &= -i g_{\mu\nu} (\delta_{ab} \delta_{cd} - \delta_{ad} \delta_{bc}) \\ i\Gamma_{A_a^\mu(p_1) \bar{c}_b(p_2) \Theta_c^\rho(p_3)}^{(0)} &= -i \epsilon_{abc} g_{\mu\nu} & i\Gamma_{A_a^\mu(p_1) c_b(p_2) A_c^{*\nu}(p_3)}^{(0)} &= -i \epsilon_{abc} g_{\mu\nu} & i\Gamma_{c_a(p_1) \phi_b(p_2) \phi_c(p_3) \phi_d^*(p_4)}^{(0)} &= \frac{i}{2v} \delta_{ad} \delta_{bc} \\ i\Gamma_{\phi_a(p_1) \phi_b(p_2) K_0(p_3)}^{(0)} &= -\frac{i}{v} \delta_{ab}. \end{aligned}$$

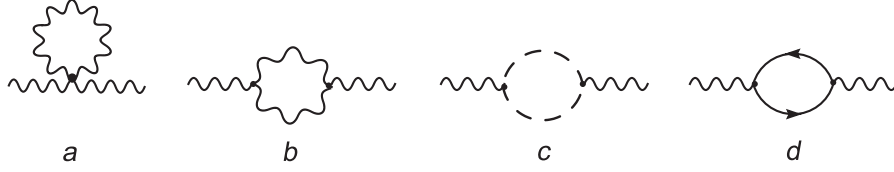


FIG. 5. Graphs contributing to the 2-point vector meson amplitude.

(i) $\Gamma^{(1)}[AA]$:

The relevant graphs are depicted in Fig. 5.

Graph (a)

$$\frac{9}{2} \frac{1}{(4\pi)^2} \frac{1}{D-4} M^2 \int d^D x A^2. \quad (\text{B1})$$

Graph (b)

$$\begin{aligned} & -6 \frac{1}{(4\pi)^2} \frac{1}{D-4} M^2 \int d^D x A^2 - \frac{25}{6} \frac{1}{(4\pi)^2} \frac{1}{D-4} \\ & \times \int d^D x \partial_\mu A_{a\nu} \partial^\mu A_a^\nu + \frac{14}{3} \frac{1}{(4\pi)^2} \frac{1}{D-4} \\ & \times \int d^D x \partial A_a \partial A_a. \end{aligned} \quad (\text{B2})$$

Graph (c)

$$\frac{1}{12} \frac{1}{(4\pi)^2} \frac{1}{D-4} \int d^D x (\partial_\mu A_{a\nu} \partial^\mu A_a^\nu - \partial A_a^2). \quad (\text{B3})$$

Graph (d)

$$-\frac{1}{6} \frac{1}{(4\pi)^2} \frac{1}{D-4} \int d^D x (\partial_\mu A_{a\nu} \partial^\mu A_a^\nu + 2\partial A_a^2). \quad (\text{B4})$$

(ii) $\Gamma^{(1)}[AAA]$:

The relevant graphs are depicted in Fig. 6.

Graph (a)

$$-\frac{15}{2} \frac{1}{(4\pi)^2} \frac{1}{D-4} \int d^D x \epsilon_{abc} \partial_\mu A_{a\nu} A_b^\mu A_c^\nu. \quad (\text{B5})$$

Graph (b)

$$2 \frac{1}{(4\pi)^2} \frac{1}{D-4} \int d^D x \epsilon_{abc} \partial_\mu A_{a\nu} A_b^\mu A_c^\nu. \quad (\text{B6})$$

Graph (c)

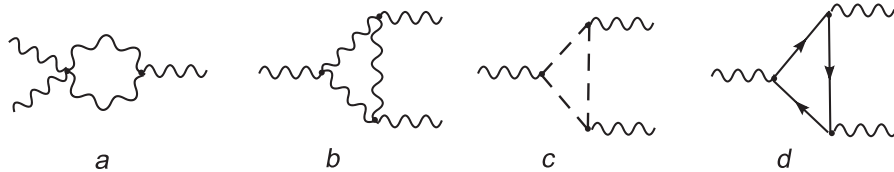


FIG. 6. Graphs contributing to the 3-point vector meson amplitude.

$$+\frac{1}{12} \frac{1}{(4\pi)^2} \frac{1}{D-4} \int d^D x \epsilon_{abc} \partial_\mu A_{a\nu} A_b^\mu A_c^\nu. \quad (\text{B7})$$

Graph (d)

$$-\frac{1}{6} \frac{1}{(4\pi)^2} \frac{1}{D-4} \int d^D x \epsilon_{abc} \partial_\mu A_{a\nu} A_b^\mu A_c^\nu. \quad (\text{B8})$$

(iii) $\Gamma^{(1)}[AAAA]$:

The relevant graphs are depicted in Fig. 7.

Graph (a)

$$-\frac{1}{(4\pi)^2} \frac{1}{D-4} \int d^D x \left[\frac{49}{24} (A^2)^2 + \frac{1}{12} (A_{a\mu} A_b^\mu) (A_{a\nu} A_b^\nu) \right]. \quad (\text{B9})$$

Graph (b)

$$\frac{1}{(4\pi)^2} \frac{1}{D-4} \int d^D x \left[\frac{7}{3} (A^2)^2 + \frac{8}{3} (A_{a\mu} A_b^\mu) (A_{a\nu} A_b^\nu) \right]. \quad (\text{B10})$$

Graph (c)

$$-\frac{1}{(4\pi)^2} \frac{1}{D-4} \int d^D x [(A^2)^2 + 2(A_{a\mu} A_b^\mu) (A_{a\nu} A_b^\nu)]. \quad (\text{B11})$$

Graph (d)

$$-\frac{1}{(4\pi)^2} \frac{1}{D-4} \int d^D x \left[\frac{1}{48} (A^2)^2 + \frac{1}{24} (A_{a\mu} A_b^\mu) (A_{a\nu} A_b^\nu) \right]. \quad (\text{B12})$$

Graph (e)

$$\frac{1}{(4\pi)^2} \frac{1}{D-4} \int d^D x \left[\frac{1}{24} (A^2)^2 + \frac{1}{12} (A_{a\mu} A_b^\mu) (A_{a\nu} A_b^\nu) \right]. \quad (\text{B13})$$

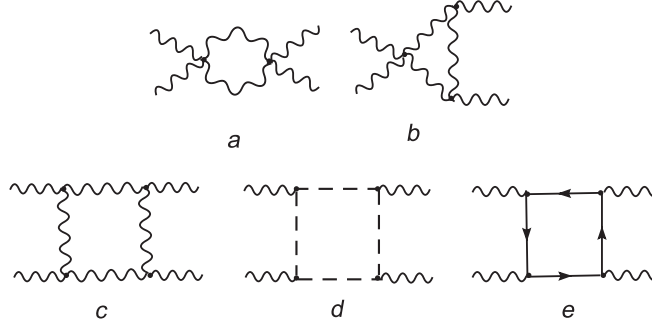


FIG. 7. Graphs contributing to the 4-point vector meson amplitude.

 (iv) $\Gamma^{(1)}[VA]$:

The relevant graphs are depicted in Fig. 8.

Graph (a)

$$3 \frac{1}{(4\pi)^2} \frac{1}{D-4} \int d^D x M^2 V_{a\mu} A_a^\mu + \frac{8}{3} \frac{1}{(4\pi)^2} \frac{1}{D-4} \times \int d^D x V_{a\mu} \square A_a^\mu - \frac{5}{3} \frac{1}{(4\pi)^2} \frac{1}{D-4} \int d^D x V_{a\mu} \partial^\mu \partial A_a. \quad (\text{B14})$$

Graph (b)

$$+ \frac{1}{3} \frac{1}{(4\pi)^2} \frac{1}{D-4} \int d^D x [V_{a\mu} (\square A_a^\mu - 4\partial^\mu \partial A_a)]. \quad (\text{B15})$$

 (v) $\Gamma^{(1)}[VAA]$:

The relevant graphs are depicted in Fig. 9.

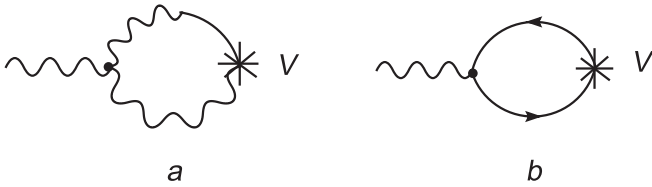
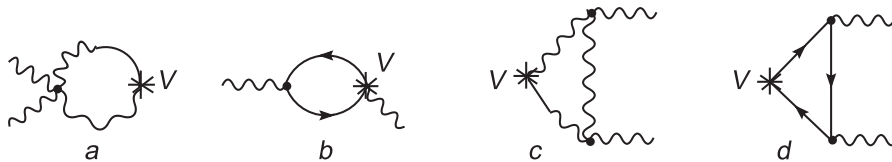

 FIG. 8. Graphs contributing to the 2-point mixed background gauge-vector gauge amplitude. The wavy-solid line is the BA -propagator.


FIG. 9. Graphs contributing to the one background gauge and two vector meson legs.

Graph (a)

$$\frac{3}{2} \frac{1}{(4\pi)^2} \frac{1}{D-4} \int d^D x (\epsilon_{abc} V_{a\mu} \partial A_b A_c^\mu - \epsilon_{abc} V_{a\mu} \partial_\nu A_b^\mu A_c^\nu). \quad (\text{B16})$$

Graph (b)

$$\frac{1}{(4\pi)^2} \frac{1}{D-4} \int d^D x \epsilon_{abc} V_{a\mu} \partial A_b A_c^\mu. \quad (\text{B17})$$

Graph (c)

$$\frac{1}{(4\pi)^2} \frac{1}{D-4} \int d^D x \left(\frac{1}{3} \epsilon_{abc} V_{a\mu} \partial A_b A_c^\mu - \frac{25}{6} \epsilon_{abc} V_{a\mu} \partial_\nu A_b^\mu A_c^\nu + \frac{17}{6} \epsilon_{abc} V_{a\mu} \partial^\mu A_{b\nu} A_c^\nu \right). \quad (\text{B18})$$

Graph (d)

$$\frac{1}{(4\pi)^2} \frac{1}{D-4} \int d^D x \left(\frac{1}{6} \epsilon_{abc} V_{a\mu} \partial A_b A_c^\mu - \frac{1}{3} \epsilon_{abc} V_{a\mu} \partial_\nu A_b^\mu A_c^\nu + \frac{1}{6} \epsilon_{abc} V_{a\mu} \partial^\mu A_{b\nu} A_c^\nu \right). \quad (\text{B19})$$

 (vi) $\Gamma^{(1)}[VAAA]$:

The relevant graphs are depicted in Fig. 10.

Graph (a)

$$- \frac{1}{(4\pi)^2} \frac{1}{D-4} \int d^D x \left(4V_{a\mu} A_a^\mu A^2 - \frac{5}{2} V_{a\mu} A_b^\mu A_{a\nu} A_b^\nu \right). \quad (\text{B20})$$

Graph (b)

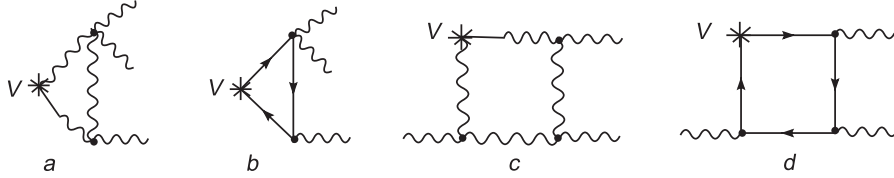


FIG. 10. Graphs contributing to the one background gauge and three vector meson legs.

$$-\frac{1}{(4\pi)^2} \frac{1}{D-4} \int d^D x \left(\frac{1}{2} V_{a\mu} A_a^\mu A^2 + \frac{1}{2} V_{a\mu} A_b^\mu A_{a\nu} A_b^\nu \right). \quad (\text{B21})$$

Graph (c)

$$\frac{1}{(4\pi)^2} \frac{1}{D-4} \int d^D x \left(\frac{4}{3} V_{a\mu} A_a^\mu A^2 + \frac{2}{3} V_{a\mu} A_b^\mu A_{a\nu} A_b^\nu \right). \quad (\text{B22})$$

Graph (d)

$$\frac{1}{(4\pi)^2} \frac{1}{D-4} \int d^D x \left(\frac{1}{6} V_{a\mu} A_a^\mu A^2 + \frac{1}{3} V_{a\mu} A_b^\mu A_{a\nu} A_b^\nu \right). \quad (\text{B23})$$

(vii) Amplitudes involving an A^* leg:
The relevant graphs are depicted in Fig. 11.

Graph (a)

$$-3 \frac{1}{(4\pi)^2} \frac{1}{D-4} \int d^D x A_{a\mu}^* \Theta_a^\mu. \quad (\text{B24})$$

Graph (b)

$$3 \frac{1}{(4\pi)^2} \frac{1}{D-4} \int d^D x A_{a\mu}^* \partial^\mu c_a. \quad (\text{B25})$$

Graph (c)

$$\frac{3}{2} \frac{1}{(4\pi)^2} \frac{1}{D-4} \int d^D x \epsilon_{abc} A_{a\mu}^* V_b^\mu c_c. \quad (\text{B26})$$

Graph (d)

$$\frac{3}{2} \frac{1}{(4\pi)^2} \frac{1}{D-4} \int d^D x \epsilon_{abc} A_{a\mu}^* V_b^\mu c_c. \quad (\text{B27})$$

(viii) Amplitudes involving K_0 , ϕ^* :
The relevant graphs are depicted in Fig. 12.

Graph (a)

$$-\frac{3v^2}{32M^4} \frac{1}{(4\pi)^2} \frac{1}{D-4} \int d^D x K_0^2. \quad (\text{B28})$$

Graph (b)

$$\frac{3v^2}{32M^4} \frac{1}{(4\pi)^2} \frac{1}{D-4} \int d^D x K_0 c_a \phi_a^*. \quad (\text{B29})$$

Graph (c)

$$-\frac{3v^2}{128M^4} \frac{1}{(4\pi)^2} \frac{1}{D-4} \int d^D x c_a \phi_a^* c_b \phi_b^*. \quad (\text{B30})$$

Graph (d)

$$-\frac{v}{8M^2} \frac{1}{(4\pi)^2} \frac{1}{D-4} \int d^D x K_0 A^2. \quad (\text{B31})$$

Graph (e)

$$\frac{v}{16M^2} \frac{1}{(4\pi)^2} \frac{1}{D-4} \int d^D x c_a \phi_a^* A^2. \quad (\text{B32})$$

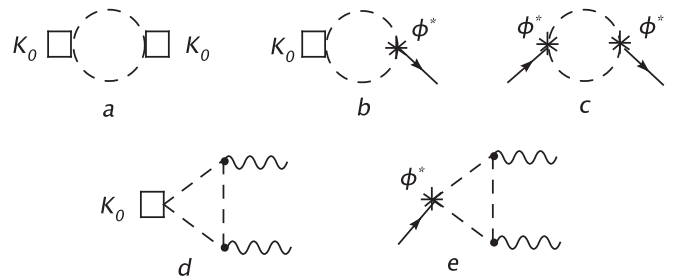


FIG. 12. Graphs with K_0 and ϕ^* legs.

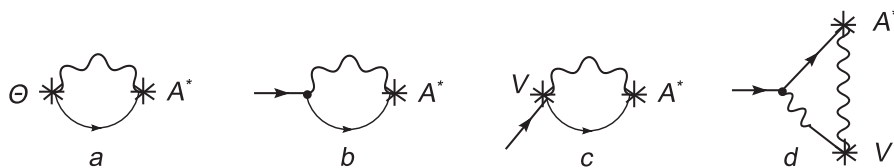


FIG. 11. Graphs with an A^* leg.

APPENDIX C: ST IDENTITY FOR THE 2-POINT VECTOR MESON AMPLITUDE

In this Appendix, we check the ST identity for the longitudinal part Σ_L of the 2-point vector meson amplitude.

Differentiation of the ST identity

$$\mathcal{S}(\Gamma) = \int d^D x \left[\frac{g^2}{\Lambda^{(D-4)}} \left(\frac{\delta\Gamma}{\delta A_{a\mu}^*} \frac{\delta\Gamma}{\delta A_a^\mu} + \frac{\delta\Gamma}{\delta \phi_a^*} \frac{\delta\Gamma}{\delta \phi_a} + \frac{\delta\Gamma}{\delta c_a^*} \frac{\delta\Gamma}{\delta c_a} \right) + B_a \frac{\delta\Gamma}{\delta \bar{c}_a} + \Theta_{a\mu} \frac{\delta\Gamma}{\delta V_{a\mu}} - K_0 \frac{\delta\Gamma}{\delta \phi_0^*} \right] = 0 \quad (\text{C1})$$

with respect to c , A_μ yields at one loop (after setting fields and external sources to zero)

$$\begin{aligned} & \Gamma_{c_b(-p)A_{c\nu}^*(p)}^{(0)} \Gamma_{A_{c\nu}(-p)A_{a\mu}(p)}^{(1)} + \Gamma_{c_b(-p)A_{c\nu}^*(p)}^{(1)} \Gamma_{A_{c\nu}(-p)A_{a\mu}(p)}^{(0)} \\ & + \Gamma_{c_b(-p)\phi_c^*(p)}^{(0)} \Gamma_{\phi_c(-p)A_{a\mu}(p)}^{(1)} + \Gamma_{c_b(-p)\phi_c^*(p)}^{(1)} \Gamma_{\phi_c(-p)A_{a\mu}(p)}^{(0)} = 0. \end{aligned} \quad (\text{C2})$$

By explicit computation one finds

$$\begin{aligned} \Gamma_{\phi_b(-p)A_{a\mu}(p)}^{(1)} &= 0, \quad \Gamma_{c_b(-p)\phi_a^*(p)}^{(1)} = 0, \\ \Gamma_{c_b(-p)A_{a\mu}^*(p)}^{(1)} &= \delta_{ab} p^\mu \left[\frac{1}{2M^2 p^2} (p^2 + M^2) H_1(M^2) \right. \\ & \quad \left. + \frac{p^2}{2M^2} H_2(0, 0) - \frac{(p^2 - M^2)^2}{2M^2 p^2} H_2(0, M^2) \right]. \end{aligned} \quad (\text{C3})$$

Moreover

$$\begin{aligned} \Gamma_{A_{b\nu}(-p)A_{a\mu}(p)}^{(0)} &= \delta_{ab} [(-p^2 + M^2) T_{\mu\nu} + M^2 L_{\mu\nu}], \\ \Gamma_{c_b(-p)A_{c\nu}^*(p)}^{(0)} \Gamma_{A_{c\nu}(-p)A_{a\mu}(p)}^{(1)} &= \delta_{ab} i p^\mu \Sigma_L. \end{aligned} \quad (\text{C4})$$

By using Eqs. (C3) and (C4) and the result in Eq. (7) for Σ_L , one sees that Eq. (C2) is fulfilled.

-
- [1] D. Bettinelli, R. Ferrari, and A. Quadri, Phys. Rev. D **77**, 045021 (2008).
- [2] C. N. Yang and R. L. Mills, Phys. Rev. **96**, 191 (1954).
- [3] M. J. G. Veltman, Nucl. Phys. **B7**, 637 (1968).
- [4] A. A. Slavnov, Theor. Math. Phys. **10**, 201 (1972).
- [5] R. Ferrari, M. Picariello, and A. Quadri, Phys. Lett. B **611**, 215 (2005).
- [6] R. Ferrari, J. High Energy Phys. **08** (2005) 048.
- [7] R. Ferrari and A. Quadri, Int. J. Theor. Phys. **45**, 2497 (2006).
- [8] R. Ferrari and A. Quadri, J. High Energy Phys. **01** (2006) 003.
- [9] D. Bettinelli, R. Ferrari, and A. Quadri, Int. J. Mod. Phys. A **23**, 211 (2008).
- [10] D. Bettinelli, R. Ferrari, and A. Quadri, J. High Energy Phys. **03** (2007) 065.
- [11] A. A. Slavnov, Theor. Math. Phys. **10**, 99 (1972) [Teor. Mat. Fiz. **10**, 153 (1972)]; J. C. Taylor, Nucl. Phys. **B33**, 436 (1971).
- [12] G. Curci and R. Ferrari, Nuovo Cimento Soc. Ital. Fis. **35A**, 273 (1976); T. Kugo and I. Ojima, Phys. Lett. **73B**, 459 (1978).
- [13] R. Ferrari and A. Quadri, J. High Energy Phys. **11** (2004) 019.
- [14] P. W. Higgs, Phys. Lett. **12**, 132 (1964); Phys. Rev. Lett. **13**, 508 (1964); Phys. Rev. **145**, 1156 (1966); F. Englert and R. Brout, Phys. Rev. Lett. **13**, 321 (1964); G. S. Guralnik, C. R. Hagen, and T. W. B. Kibble, Phys. Rev. Lett. **13**, 585 (1964); T. W. B. Kibble, Phys. Rev. **155**, 1554 (1967).
- [15] W. J. Marciano and A. Sirlin, Phys. Rev. D **22**, 2695 (1980); **31**, 213(E) (1985).
- [16] G. 't Hooft, Nucl. Phys. **B33**, 173 (1971).
- [17] M. J. Herrero and E. Ruiz Morales, Nucl. Phys. **B437**, 319 (1995); **B418**, 431 (1994); S. Dittmaier and C. Grosse-Knetter, Nucl. Phys. **B459**, 497 (1996).
- [18] S. Dittmaier and C. Grosse-Knetter, Phys. Rev. D **52**, 7276 (1995).
- [19] K. i. Shizuya, Nucl. Phys. **B121**, 125 (1977).
- [20] Yu. N. Kafiev, Nucl. Phys. **B201**, 341 (1982).